
APPLIED PROBLEMS
OF STRENGTH AND PLASTICITY

Degradation and Failure of Pipes from an Oil-and-Gas Pipeline in Media with a High Content of Carbon Dioxide and Chlorine Ions

M. A. Vyboishchik^a, A. V. Ioffe^b, T. V. Tetyueva^b, V. A. Revyakin^b, and I. V. Gruzkov^b, *

^aTogliatti State University, Tolyatti, 445020 Russia

^bOOO IT-Servis, Samara, 443001 Russia

*e-mail: gruzkov@its-samara.com

Received December 2, 2019; revised December 2, 2019; accepted December 18, 2019

Abstract—Field (bypass) tests of the pipes made of 09G2S, 13KhFA and 08KhMFA steels are carried out under the conditions of the operating oil pipeline in the Priobskoye deposit with a high content of CO₂ and Cl⁻. The test period is two years. The medium composition initiates intense carbon dioxide corrosion in a local aggressive form. Corrosion damages have a complex volumetric configuration and consist of numerous channels. The local corrosion rate is more than four times higher than the general corrosion rate. According to an increase in the corrosion resistance under the operating conditions, the steels under study are arranged in the following sequence: 09G2S → 13KhFA → 08KhMFA.

Keywords: oilfield media, field (bypass) tests, corrosion failure, carbon dioxide corrosion, structural state, corrosion products

DOI: 10.1134/S0036029520100328

1. INTRODUCTION

The constant increase in the activity of the produced media and the use of methods for intensifying oil production accelerate the processes of corrosion failure, especially local corrosion failure (pitting corrosion, grooving corrosion). The main causes of the degradation and failure of oil production equipment in most deposits of our country (in particular, Volga region, Western and Eastern Siberia) are carbon dioxide corrosion induced by a high content of carbon dioxide and chlorine and the absence of preventive corrosion protection measures [1, 2]. Practice demonstrated the efficiency of using chrome-alloyed steel pipes in such media. It should be taken into account that an increase in the chromium content from 2 to 13% leads, in addition to a significant increase in the cost, to a decrease in the mechanical properties and the resistance to sulfide stress corrosion cracking [3–5]. Other solutions, which are based on the optimization of the composition (without high alloying) and the structural state, are needed. Their implementation requires systematic testing of pipe steels, which differ in composition and structure.

Currently, there are no generally accepted methods for laboratory carbon dioxide corrosion resistance tests of pipes. Accordingly, the test results obtained in different laboratories can be slightly comparable and differ from the results of field tests. Field tests, where the coils of the pipes under study are installed in a bypass (bypass) line of an operating pipeline, can be

considered as close as possible to real pipe operation conditions.

Despite numerous studies of the internal corrosion of industrial pipelines [6–8], the mechanisms of initiation and development of carbon dioxide corrosion and the factors that determine the process intensity and the probability of transition to more aggressive local forms are poorly understood. The purpose of this work is to find the mechanism and kinetics of the development of carbon dioxide corrosion in oil-and-gas pipes in deposits with a high content of carbon dioxide and chlorine ions.

2. EXPERIMENTAL

2.1. Materials

Pipes from 13KhFA and 08KhMFA steels were tested and compared with pipes made of traditional 09G2S steel. The pipe diameter was 159 mm and the wall thickness was 8 mm. The chemical compositions of the steels are given in Table 1.

The pipes made of 09G2S steel of strength class K50 were normalized from 900°C, which led to the formation of a ferrite–pearlite microstructure. The pipes made of 13KhFA and 08KhMFA steels were quenched from temperatures above A_{c3} (920°C), then quenched from the intercritical A_{c3}–A_{c1} temperature range (770°C), and tempered at 600°C. Double quenching provides finer grains, a better structure homogeneity, a higher ductility (Table 2), and

Table 1. Chemical compositions of the steels, wt %

Steel	C	Si	Mn	Al	Cr	Mo	V	Ni	Cu	P	S
13KhFA	0.14	0.36	0.55	0.043	0.57	0.012	0.052	0.09	0.13	0.013	0.002
08KhMFA	0.11	0.31	0.53	0.031	0.62	0.128	0.044	0.14	0.23	0.008	0.006
09G2S	0.10	0.55	1.33	—	0.13	—	—	0.13	0.16	0.011	0.008

Table 2. Mechanical properties of the pipe metal

Steel	σ_u , MPa	σ_y , MPa	δ , %	Fracture toughness, J/cm ² and fraction of ductile component in fracture, % at test temperature							
				−40°C		−50°C		−60°C		−70°C	
				KCV	D	KCV	D	KCV	D	KCV	D
13KhFA	592	421	32.4	231	100	229	100	224	100	203	90
08KhMFA	665	506	20.4	291	100	288	100	276	100	263	100
09G2S	520	370	29.0	257	100	254	100	245	100	217	100

increased corrosion resistance as compared to conventional quenching from the austenitic region with subsequent high tempering [9–12]. These pipes belong to strength class K52–K54 and are characterized by high cold resistance, fracture toughness (see Table 2), and resistance to hydrogen cracking and sulfide corrosion stress cracking.

The microstructure of the pipes made of 13KhFA and 08KhMFA steels is identical in morphology (Fig. 1), is homogeneous across the wall thickness, and is represented by ferrite grains having precipitated on quenching from a temperature from the intercritical range and grains of a ferrite–carbide mixture formed during the decomposition of bainite structures. The fraction of ferrite is $\approx 65\%$. The carbide precipitates have a rounded shape and are located both along the boundaries and inside ferrite grains. No banded structure of the metal was revealed. The grain size in the 13KhFA pipe steel is 10–12 μm for ferrite and at most 17 μm for a ferrite–carbide mixture. The

grain size in the 08KhMFA steel is usually smaller by 15–20%.

2.2. Investigation Techniques

The studies were carried out at the test site of the Priobskoye deposit in Western Siberia, the oilfield media of which are characterized by a high activity. During the period under study, the CO_2 partial pressure was $p_{\text{CO}_2} = 103.3$ kPa, the salinity was 48.3 g/L, and the content of chloride ions was 27.0 g/L (Table 3). It should be noted that chlorides significantly intensify the development of carbon dioxide corrosion [2], and their combination with a high CO_2 content, salinity, and water cut of the medium lead to very severe conditions for the operation and testing of oilfield pipes.

The test section consisted of an operating oil pipeline made of 09G2S steel pipes and a parallel bypass line composed of successively arranged coils of pipes made of 13KhFA and 08KhMFA steels mounted with

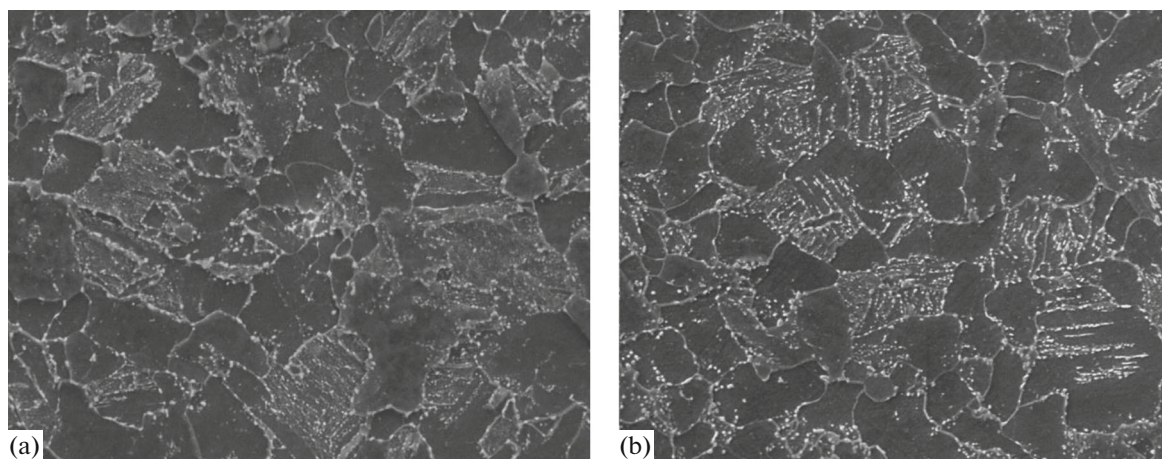
**Fig. 1.** Microstructure of (a) 13KhFA and (b) 08KhMFA steels. Scanning electron microscopy, $\times 5000$.

Table 3. Characteristics of the transported medium

Temperature, °C	H ₂ O, %	P_{\max}^* , MPa	P_{CO_2} , kPa	pH	H ₂ S, mg/L	Ionic composition of water phase, g/L						Salinity, g/L
						Ca ²⁺	Mg ²⁺	K ⁺ + Na ⁺	Cl ⁻	SO ₄ ²⁻	HCO ₃ ³⁻	
56	86	1.2	103.2	5.9	20	0.75	0.12	18.4	27.0	0.77	1.37	48.3

* Working press in pipeline.

Table 4. General corrosion rate (data of two-year field tests)

Steel	Corrosion thinning of pipe wall, mm		General corrosion rate, mm/year	
	max	av.	max	av.
13KhFA	0.81	0.54	0.39	0.26
08KhMFA	0.68	0.42	0.33	0.20

flanges. The tests were carried out for two years, after which the coils were dismantled, cut, and cleaned of oil products.

The state of the outer and inner surfaces of the pipes was studied by metallographic analysis. The thinning of the pipe wall as a result of corrosion was determined according to the readings of an ultrasonic thickness gauge, and the general corrosion rate was calculated. The pipe wall measurements were carried out before and after the tests using a preliminarily applied grid in three parallel planes (eight points every 45° in each plane and five measurements at each

point). X-ray diffraction (XRD) analysis of the corrosion products on the inner surface of the pipes was carried out using a Dron-3 X-ray diffractometer. The morphology and chemical composition of the corrosion products were studied on metallographic micro-sections using a Philips scanning electron microscope with an EDAX energy dispersive analyzer. To study the mechanism of damage to the near-surface layer of pipes in contact with the transported medium, we used the method of layer-by-layer grinding of layers parallel to the inner pipe surface.

3. RESULTS AND DISCUSSION

The 09G2S steel pipes undergo intense corrosion damage (Fig. 2), and the corrosion rate along the lower generatrix of the pipe exceeds 1.5 mm/year. In contrast to this, the maximum general corrosion rate of the pipes made of 13KhFA and 08KhMFA steels is approximately 0.4 mm/year (Table 4). Their more significant corrosion damage manifests itself in a local form. In particular, round pits 5–7 mm in diameter are detected on the inner surface of the tubes (Fig. 3). The number of pits on the 13KhFA steel the pipes is larger, they are located close to each other, and some

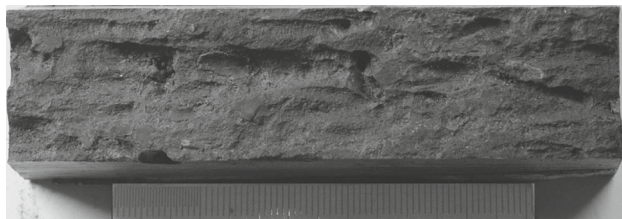


Fig. 2. Inner surface of pipe made of 09G2S steel, lower generatrix of the pipe.

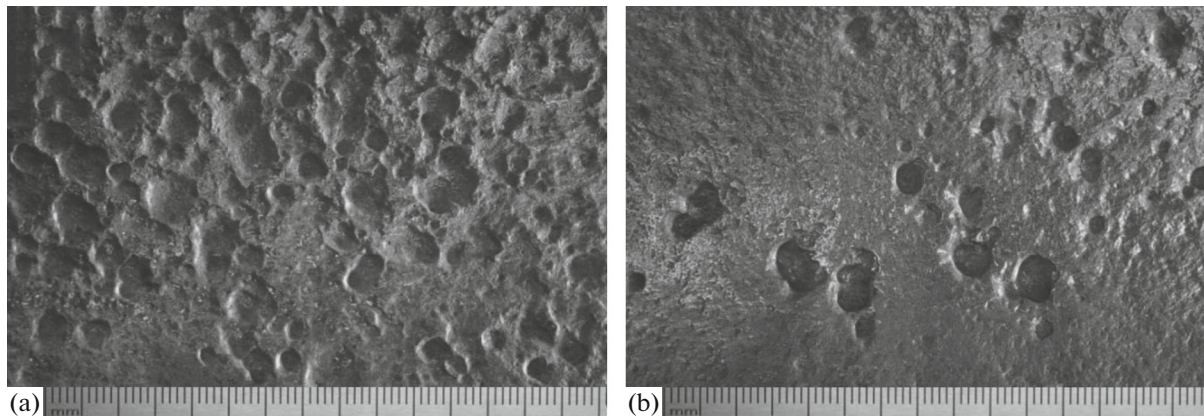


Fig. 3. Inner pipe surface cleaned from deposits after tests: (a) 13KhFA steel and (b) 08KhMFA steel.

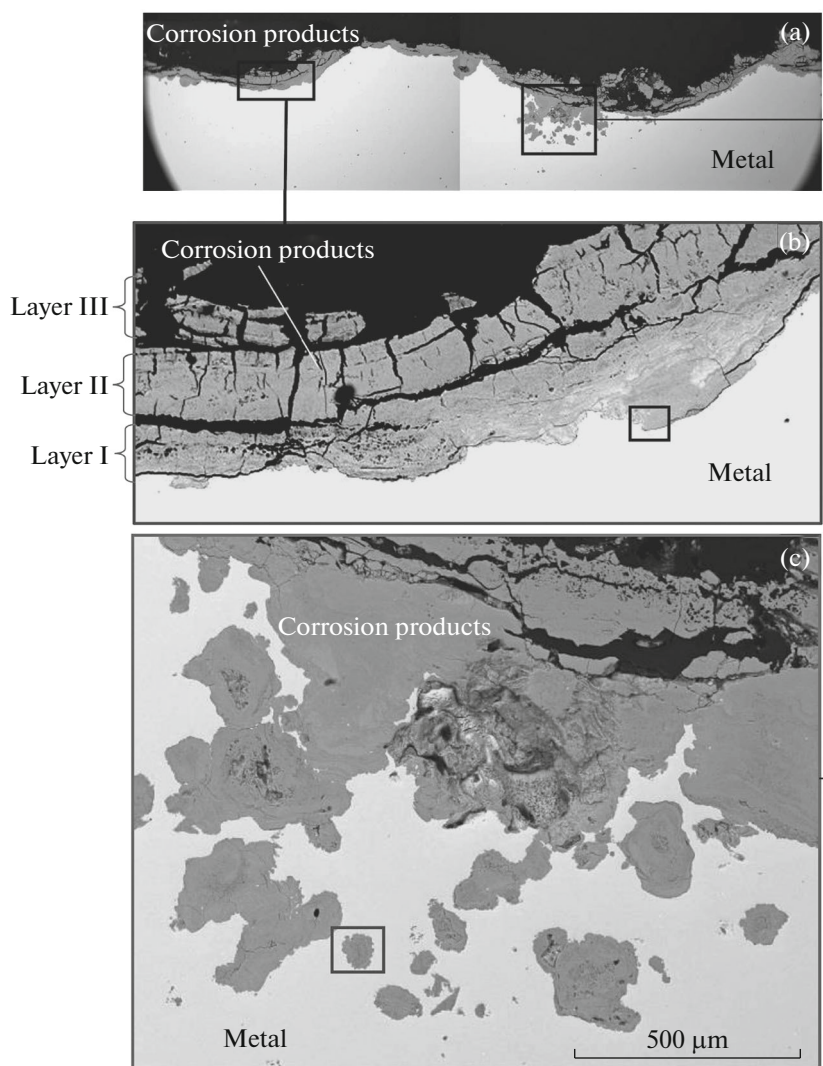


Fig. 4. Corrosion damage and the corrosion products in 13KhFA steel pipes: (a) general view, (b) general corrosion region, and (c) accelerated local corrosion region.

ulcers are unified (see Fig. 3a). The number of pits on the surface of the 08KhMFA steel pipes is significantly smaller (see Fig. 3b).

As shown by XRD analysis, the main constituent of the corrosion products is represented by iron carbonates (FeCO_3), and, accordingly, the predominant damage mechanism is carbon dioxide corrosion. In addition to iron carbonates, the corrosion layer contains a certain amount of alloying elements (Cr, Si, Mo) in the form of hydrated compounds. The chromium content in the corrosion products is 5–10 times higher than in steel [10, 13]. The carbide phase of the steels does not interact with aggressive oilfield media and passes to corrosion products, preserving the arrangement of carbides. A layer of corrosion products forms: it is complex in structure and composition and

reduces or interrupts the access of a corrosive medium to the pipe metal.

During operation, a dynamic equilibrium is established between the processes of formation and destruction of the protective layer of corrosion products, which determines the intensity of corrosion damage to the pipes. The corrosion products can be conventionally divided into several layers (Fig. 4): the lower layer, which is adjacent to the pipe metal, is denser, and the upper layers are in contact with the corrosive medium. The layers differ in the degree of damage and the number of cracks.

Accelerated local corrosion, penetrating to a depth of 2 mm, is also observed along with the general corrosion (see Figs. 4, 5). The manifestation of this corrosion is somewhat unusual. Corrosion damages of various sizes and geometries are located randomly in

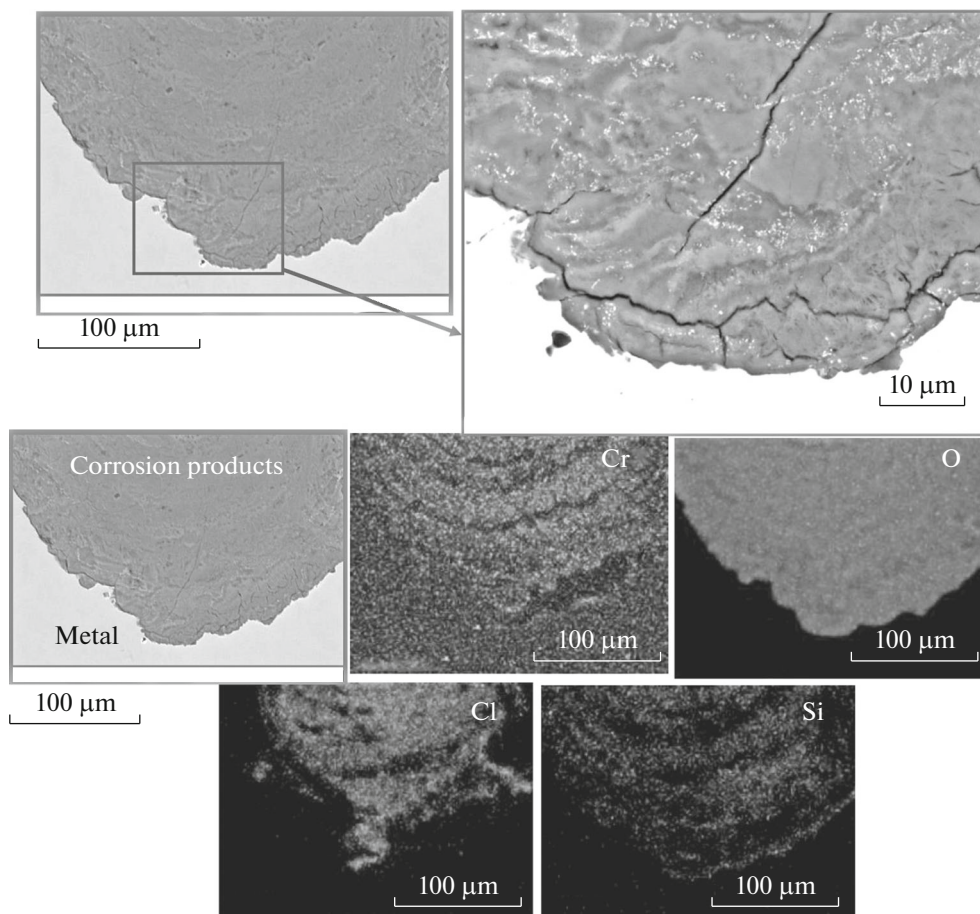


Fig. 5. Morphology and composition of (characteristic X-ray radiation) of the corrosion products from a general corrosion area in the 13KhFA steel pipe (indicated by the square in Fig. 4b).

the form of separate fragments in the near-surface layer volume. No direct contact of corrosion damage fragments with the transported medium is observed on a polished section (see Figs. 4c).

The mechanism of local accelerated corrosion is associated with the periodic formation and removal of corrosion products in some corrosive metal areas. These areas become anodes and the remaining corrosion products become cathodes. As a result, active corrosion macrocouples form on the metal surface, leading to the dissolution of the anode areas at an extremely high rate [14, 15]. Naturally, the process kinetics is determined by the factors causing the destruction of the corrosion product layer.

One of the causes for intensifying the destruction of the corrosion products and the appearance of local accelerated corrosion damage forms is a high content of chlorine ions in a corrosive medium. According to the existing concepts, the action of chlorine is associated with the hydrolysis of the FeCl_2 compound forming at the electrode layer; as a result, significant acidi-

fication of the medium and the accelerated dissolution of the corrosion products in these places take place in the anode steel areas [2].

The chemical composition of the corrosion products in the areas of uniform and local corrosion is identical: they consist mainly of iron and oxygen and contain a high (in relation to steel) chromium and silicon content. The identity of the corrosion product composition can also indicate the identity of the process mechanism, namely, the manifestation of carbon dioxide corrosion. Chlorine is concentrated at the interface between the corrosion products and the base metal, especially in corrosion pits (Figs. 5–7). The peculiarity of its location manifests itself in the presence of pronounced thin chloride layers, which deeply penetrate into the surrounding metal. This arrangement and effect of chlorine are likely to be due to the fact that chlorine has a larger atomic radius as compared to iron ($r_{\text{Cl}} = 1.40 \text{ \AA}$, $r_{\text{Fe}} = 1.26 \text{ \AA}$), does not dissolve in iron, and concentrates on the metal surface to

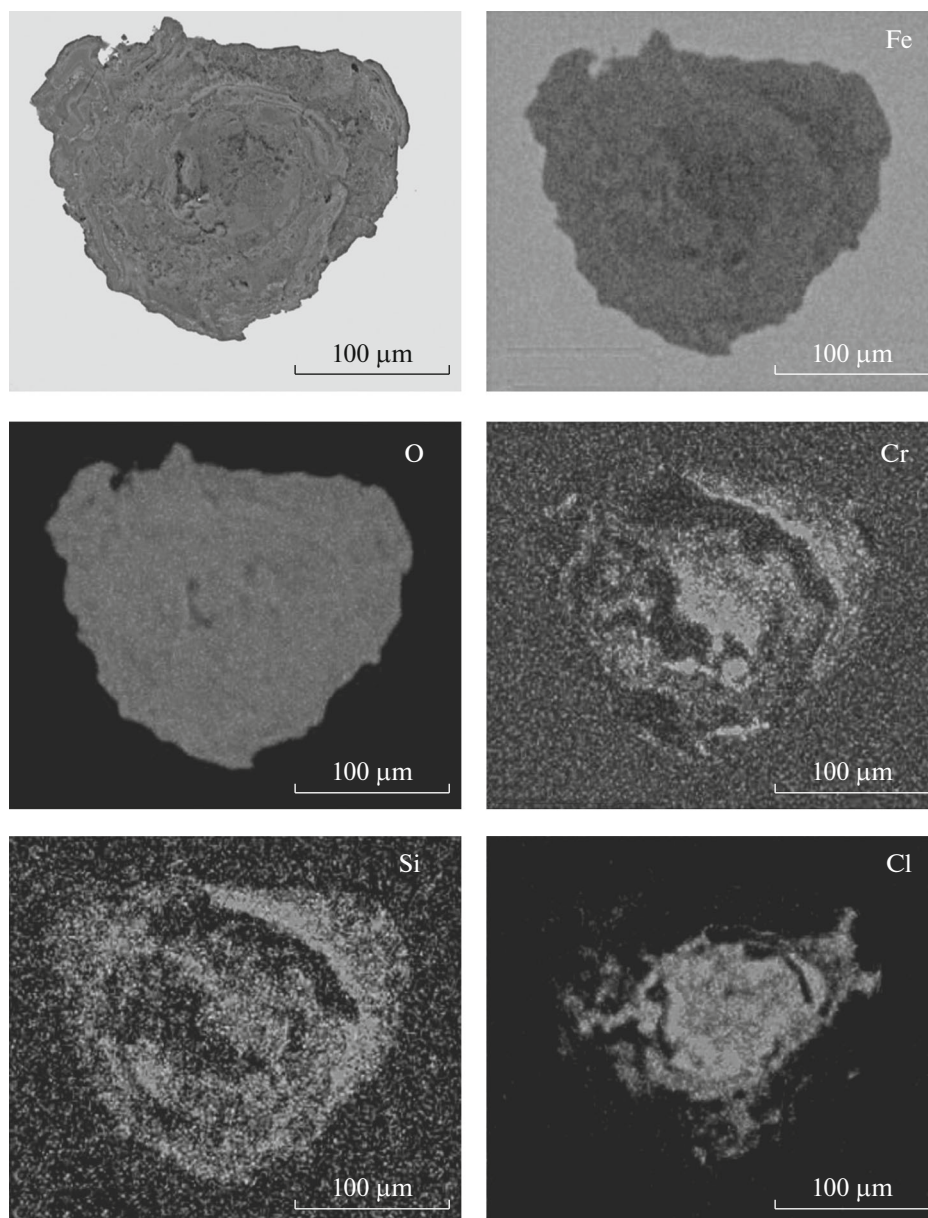


Fig. 6. Structure and composition (characteristic X-ray radiation) of the corrosion products in one of the fragments of local corrosion of the 13KhFA steel pipe (indicated by the square in Fig. 4c).

form iron chlorides, which dissolve easily and are washed out by a corrosive medium.

To study the features of local corrosion damage across the pipe thickness, we used successive grinding of thin surface layers. Figure 8 shows the change in the corrosion damage across the surface layer thickness in one of the pipe sections. The following features can be noted: smaller pits appear around large ones, individual corrosion fragments disappear and new fragments appear in other places, the main pit channels are directed deep into the metal and have numerous branches in the form of smaller channels connecting the main ones, and lateral branches in some places

have a higher growth rate as compared to the main large corrosion pits. Figure 9 shows a schematic diagram for the corrosion damage during local carbon dioxide corrosion caused by chlorine ions, which is based on the results of fractographic analysis of the surface layer in the directions parallel and perpendicular to the inner pipe surface. The extended pitting of the wall of the lower generatrix of the pipe is noteworthy.

Thus, a high content (27.0 g/L) of chlorine ions in carbon dioxide oilfield media intensifies carbon dioxide corrosion and promotes its transition to a more aggressive local form, in which individual pits coalesce to form an extended channel, i.e., a worm-hole. Local

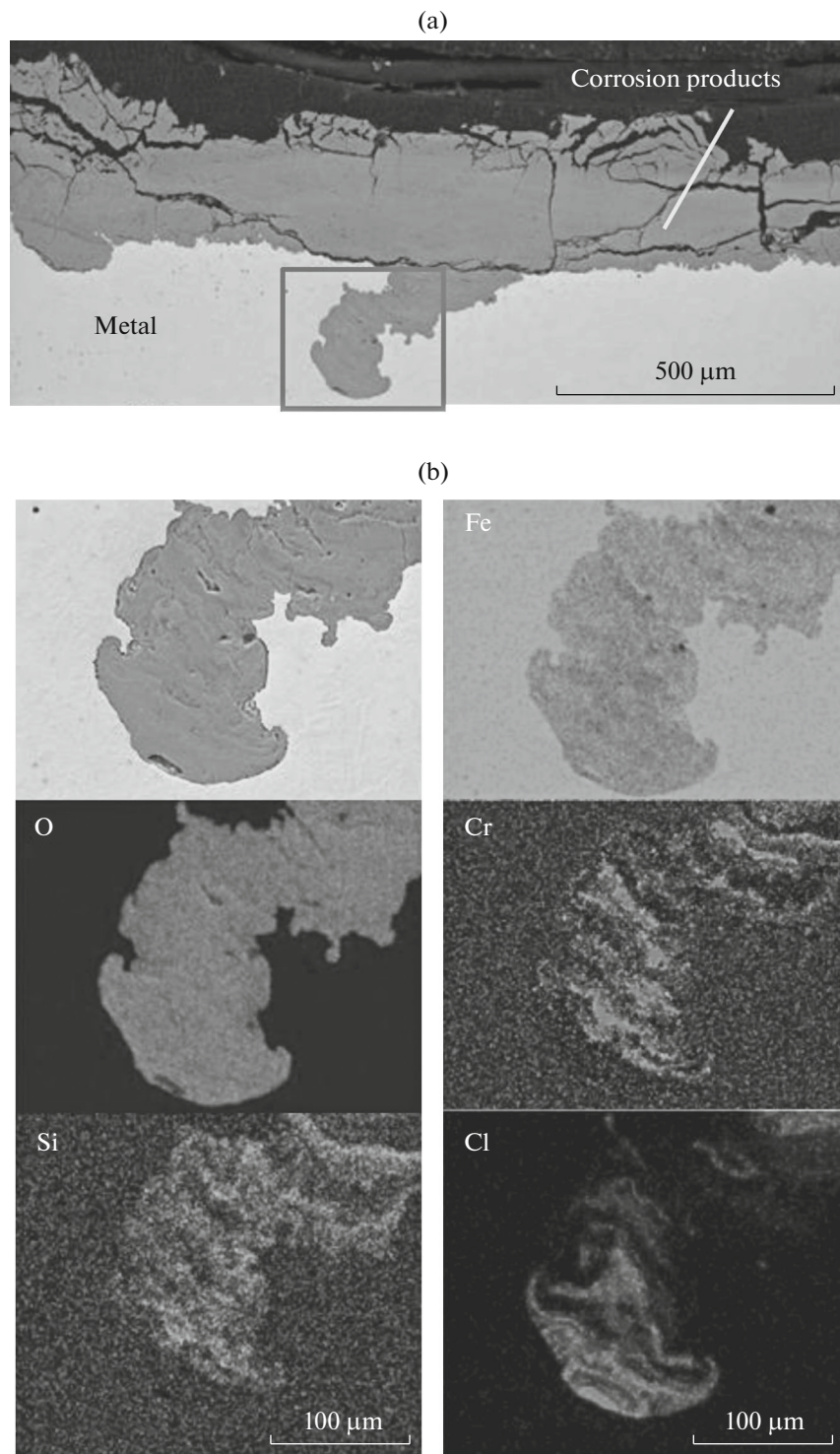


Fig. 7. Corrosion damage and the corrosion products of the 08KhMFA steel pipe: (a) general view and (b) morphology and composition (characteristic X-ray radiation) of the corrosion products in the area of accelerated local corrosion (indicated by the square in (a)).

acceleration of corrosion processes can also be caused by the action of the residues of acidic solutions (predominantly hydrochloric acid solution), which enter an oil gathering system after performing geological

and technological operations in borehole cavities. As a result, the protective layer of corrosion products on the pipe surface is destroyed with the formation of iron chloride.

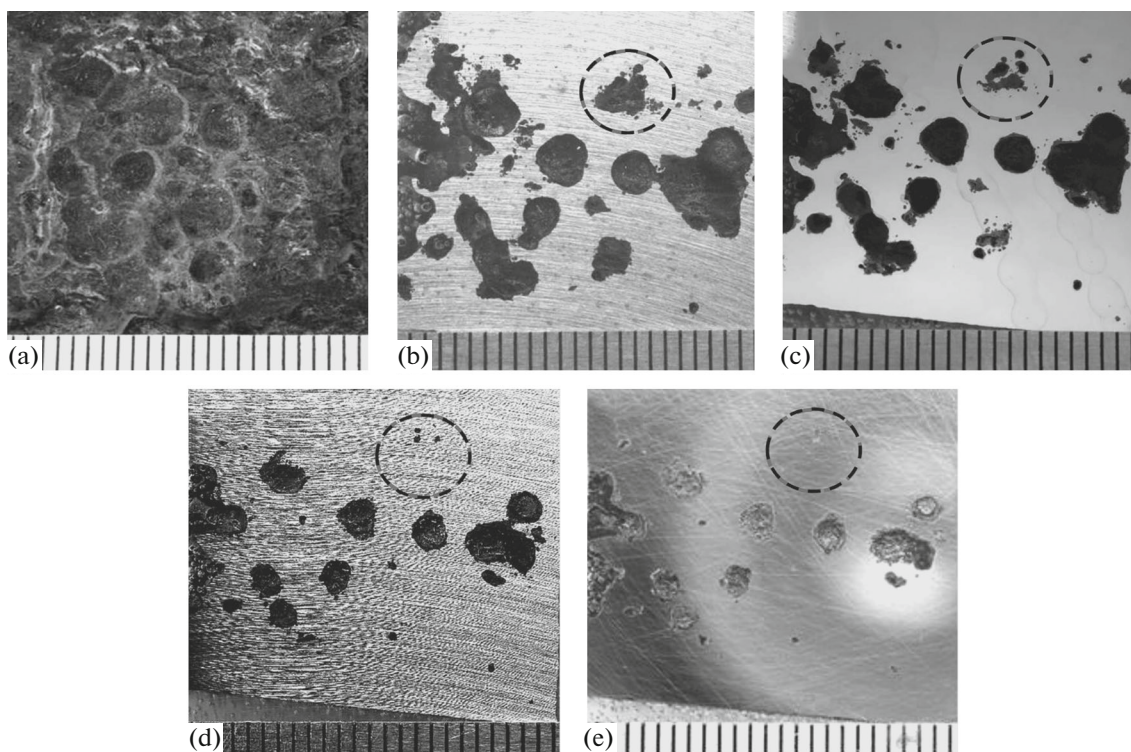


Fig. 8. Change in the corrosion damage across the near-surface layer thickness of the 13KhFA steel pipe: (a) inner pipe surface and sections at a distance of (b–e) 0.2, 0.5, 0.7, and 0.8 mm from the surface, respectively.

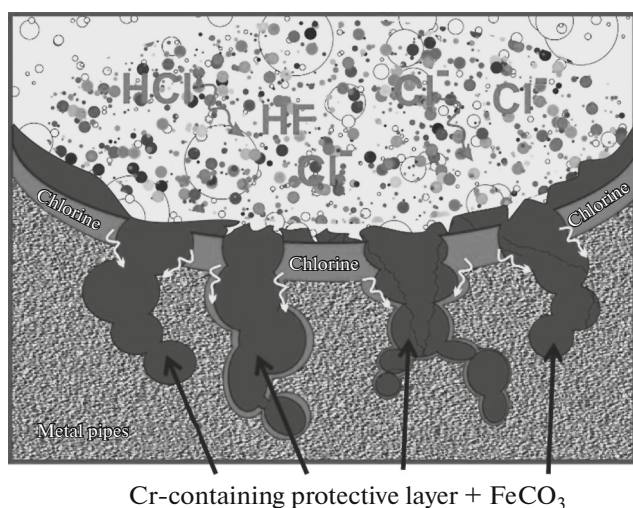


Fig. 9. Schematic view of the corrosion damage to pipes during local carbon dioxide corrosion in media with a high content of chlorine ions.

4. CONCLUSIONS

(1) Chlorine ions in places of their concentration at the metal–corrosion product interface cause intense corrosion destruction. The local corrosion rate is more than four times higher than the general corrosion rate.

(2) The corrosion damage during local carbon dioxide corrosion has a complex volumetric configuration, consists of numerous extended channels, and is similar to “wormhole” corrosion.

(3) In terms of resistance to carbon dioxide corrosion in media with a high (27.0 g/L) content of chlorine ions, the steels under study are arranged in the following sequence: 09G2S → 13KhFA → 08KhMFA. Because of intense corrosion failure, 09G2S steel is practically unsuitable for work in a carbon dioxide medium. 08KhMFA steel with a lower carbon content and additionally alloyed with molybdenum is less susceptible to local corrosion.

REFERENCES

1. V. V. Zav'yalov, *Problems of the Operational Reliability of Pipelines at the Late Stage of Field Development* (VNIIOENG, Moscow 2005).
2. A. N. Markin and R. E. Nizamov, *CO₂ Corrosion of Oil-field Equipment* (VNIIOENG, Moscow, 2003).
3. E. A. Trifonova, “Influence of alloying and structure on the corrosion-mechanical failure of pipes made of low-carbon steels in H₂S- and CO₂-containing media,” Candidate's Dissertation in Engineering (Tula, TulsU, 2010).
4. A. Ikeda, M. Ueda, and S. Mukai, “CO₂ behavior of carbon and Cr steels,” in *Proceedings of International Corrosion Forum Corrosion/85* (Boston, 1985), paper no. 29.

5. A. V. Ioffe, M. A. Vyboishchik, E. A. Trifonova, and P. V. Suvorov, "Influence of the chemical composition and structure on the carbon dioxide corrosion resistance of oil line pipes," *Metalloved. Term. Obrab. Met.*, No. 2, 9–14 (2010).
6. M. Ko, B. Ingham, N. Laycock, and D. E. Williams, "In situ synchrotron X-ray diffraction study of the effect of microstructure and boundary layer conditions on CO₂ corrosion of pipeline steels," *Corr. Sci.* **90**, 192–201 (2015).
7. Qiang Li, Haitao Hu, and Y. Frank Cheng, "Corrosion of pipelines in CO₂-saturated oil–water emulsion flow studied by electrochemical measurements and computational fluid dynamics modeling," *J. Petrol. Sci. Eng.* **147**, 408–415 (2016).
8. X. Hu and A. Neville, "CO₂ erosion–corrosion of pipeline steel (API X65) in oil and gas conditions—a systematic approach," *Wear* **267** (11), 2027–2032 (2009).
9. A. V. Ioffe, T. V. Tetyueva, V. A. Revyakin, E. A. Borisenkova, S. A. Knyaz'kin, and T. V. Denisova, "Corrosion-mechanical failure of pipe steels during operation," *Metalloved. Term. Obrab. Met.*, No. 10, 22–28 (2012).
10. M. A. Vyboishchik, A. V. Ioffe, E. A. Borisenkova, T. V. Denisova, and A. V. Sorokin, "Corrosion damage to oil line pipes made of chromium–molybdenum-containing steels under high activity of an added medium," *Metalloved. Term. Obrab. Met.*, No. 10, 29–33 (2012).
11. M. A. Vyboishchik, L. G. Marchenko, and A. I. Grekhov, "Structure and properties of pipes made of low-carbon steel after quenching from the intercritical temperature range and tempering," *Tekhn. Metall-ov*, No. 8, 2–6 (2003).
12. A. N. Makovetskii, T. I. Tabatchikova, I. L. Yakovleva, N. A. Tereshchenko, and D. A. Mirzaev, "Formation of the structure of low-alloy pipe steel in heating in the intercritical temperature range," *Fiz. Met. Metalloved.* **113** (7), 744–755 (2012).
13. M. A. Vyboishchik and A. V. Ioffe, "Development of steel resistant to carbon dioxide corrosion in oil-producing media," in *Perspektivnye Materialy* (Izd. TGU, Togliatti, 2017), Vol. VII, pp. 115–160.
14. G. Schmitt, T. Gudde, and E. Strobe-Effertz, "Fracture mechanical properties of CO₂ corrosion products scales and their relation to localized corrosion," in *Proceedings of Conference Corrosion/96* (Houston, 1996), paper no. 9.
15. T. Muraki, K. Nose, and H. Asahi, "Development of 3% chromium line pipe steel," in *Proceedings of International Corrosion Forum Corrosion 2003* (Houston, 2003), paper no. 117.

Translated by K. Shakhlevich